Research Square

Preprints are preliminary reports that have not undergone peer review.
They should not be considered conclusive, used to inform clinical practice,
or referenced by the media as validated information.

A Velocity-Independent DOA Estimator of Underwater Acoustic Signals Via An Arbitrary Cross-Linear Nested Array

Gengxin Ning
South China University of Technology
Yu Wang (wy13273819650@163.com)
South China University of Technology https://orcid.org/0000-0001-8771-3270
Guangyu Jing
South China University of Technology
Xuejin Zhao
Guangdong University of Technology

Research Article

Keywords: Underwater DOA estimation, Velocity-independent, Arbitrary Cross-linear array, Nested array

Posted Date: December 2nd, 2021

DOI: https://doi.org/10.21203/rs.3.rs-1121319/v1

License: This work is licensed under a Creative Commons Attribution 4.0 International License.
Read Full License

RESEARCH

A Velocity-independent DOA Estimator of Underwater Acoustic Signals Via an Arbitrary Cross-linear Nested Array

Gengxin Ning[1], Yu Wang[1*], Guangyu Jing[1] and Xuejin Zhao[2]

Abstract

In this paper, an estimator for underwater DOA estimation is proposed by using a cross-linear nested array with arbitrary cross angle. The estimator excludes the variation acoustic velocity by deriving the geometric relation of the cross-linear array on the proposed algorithm. Therefore, compared with traditional DOA estimation algorithms via linear array, this estimator eliminates systematic errors caused by the uncertainty factor of the acoustic velocity in the underwater environment. Compared with the traditional acoustic velocity independent algorithm, this estimator uses the nested array and improves the performance of DOA estimation. In addition, the estimator is based on arbitrary angle of the cross-linear array, so it is more flexible in practical applications. Numerical simulations are provided to validate the analytical derivations and corroborate the improved performance in underwater environments where the actual acoustic velocity is not accurate.

Keywords: Underwater DOA estimation; Velocity-independent; Arbitrary Cross-linear array; Nested array

1 Introduction

The DOA estimation algorithms have been widely used in radar, sonar, wireless communication and other fields [1, 2, 3]. DOA is also one of the important parameters of the underwater communication system [4]. Because the seawater has a great absorption of electromagnetic wave, the underwater communication system often takes acoustic wave as the main carrier of communication. In the underwater channel environment, the speed of sound is mainly affected by temperature, salinity and pressure, and it changes with these factors [5]. In general, the acoustic wave velocity ranges from $1450m/s$ to $1550m/s$, and we often can't get the accurate value at the signal sink. The traditional DOA estimation algorithm is usually based on the known acoustic velocity. The existence of the acoustic velocity error will inevitably lead to the inaccuracy of the wave path difference, and then make the DOA estimation have a systematic error. Therefore, in the process of underwater DOA estimation, it is very important to eliminate the influence of acoustic velocity error.

MUSIC algorithm [6] and ESPRIT algorithm [7] are milestone achievements in solving DOA estimation problem. They break through the Rayleigh limit of traditional beamforming algorithm and realize DOA high resolution estimation. In recent years, the ESPRIT algorithm has aroused notable research interest given that it has an advantage of low computational complexity without spectral peak search compared with the MUSIC algorithm. During this period, several improved algorithms based on ESPRIT were presented, in which realizing multi-parameter estimation, improving estimation accuracy, and reducing computational complexity are the representative aspects of research. For the first aspect mentioned, X. Wang *et al.* [8] proposed the AF-ESPRIT algorithm for joint estimation of frequency and angle, which can solve the problem of joint pairing of DOA and frequency. For the purpose of improving estimation accuracy, Pinto *et al.* [9] proposed the MS-KAI-ESPRIT algorithm. In this algorithm, a convergence factor is set, and the interference factors in the data covariance matrix are gradually eliminated by iterative method, so that the method achieves better performance under the condition of low SNR and less snapshots. In addition, Ref. [10] and [11] proposed the GLS-ESPRIT and ES-ESPRIT algorithms respectively by studying the generalized least squares problem. Both of these two algorithms transform the signal subspace model of the subarray into the mathematical model of the basic generalized least squares problem through mathemat-

*Correspondence: wy13273819650@163.com
[1] South China University of Technology, Guangzhou, China
Full list of author information is available at the end of the article

ical transformation. By solving the generalized least squares problem, the noise disturbance is suppressed, and the optimal estimation of the rotation matrix is realized, which greatly improves the estimation accuracy of the ESPRIT algorithm. To reduce complexity, Q. Cheng [12] studied the influence of the overlapping degree of submatrix on the estimation accuracy, improved ESPRIT algorithm slightly, and proposed MS-ESPRIT algorithm, which has lower computational complexity compared with other algorithms. In order to facilitate the operation of the hardware, Akkar *et al.* [13] used matrix LU decomposition or QR decomposition to replace the original eigenvalue decomposition. They, abbreviated as the LU-ESRPIT algorithm and QR-ESPRIT algorithm, made the calculation only need linear operation, convenient for engineer implementation, which reduced the computational complexity and storage cost of the processor.

All the above algorithms are based on the common uniform linear array (ULA). Yet this traditional array structure has the following disadvantages:

1) The number of identifiable sources with ULAs is limited to the number of array elements minus one;
2) The accuracy of DOA estimation is also limited by the inherent size of the array aperture;
3) Unable to deal with the DOA estimation problem in some special environments effectively, such as the underwater communication with the unknown acoustic velocity.

Therefore, in addition to improvements in data processing, scholars are also exploring the special effects of different array layouts on DOA estimation algorithms, including sparse linear array (SLA), the L-shaped array, the parallel array, etc. In Ref. [14], Z. Zheng *et al.* arranged a coprime array and constructed a Toeplitz matrix with data holes by using the data output from the array. And the Toeplitz matrix was filled and restored by solving the minimum nuclear norm problem. This method can process coherent signals and achieve high resolution estimation of DOA. In Ref. [15], L. Li *et al.* improved the traditional virtual-ESPRIT algorithm based on high-order cumulants, which does not require equal spacing of sensors and is suitable for irregular linear arrays. In Ref. [16], Van *et al.* used a sparse array in underwater acoustic DOA estimation and combined it with MUSIC algorithm to improve the accuracy of underwater DOA estimation. In references [17, 18, 19], researchers realized two-dimensional DOA estimation by taking advantage of the special geometric properties of the L-shaped or the parallel arrays. In particular, the researchers of [17] and [18] used the sparse arrays, which greatly improved the accuracy of DOA estimation. While, these algorithms developed above cannot be directly used for DOA estimation in the underwater environment, and they cannot deal with the systematic influence of acoustic velocity error in underwater environments.

To solve the problem of underwater acoustic velocity error, the reference [20] proposed a VI-MUSIC algorithm independent of acoustic velocity. By placing L-shaped arrays in the environment and setting an acoustic velocity interval, it searches the range of acoustic velocity from $1450m/s$ to $1550m/s$ to complete the preliminary estimation of acoustic velocity and eliminate the influence of acoustic velocity on DOA estimation. The FVI-ESPRIT algorithm was proposed in reference [21], which is based on arbitrary cross-linear array and makes full use of geometric relations of the cross-linear array. However, in the one-dimensional DOA estimation problem, the performance of the cross array is far inferior to the linear array, which can be verified by deriving their Cramér-Rao Bound (CRB).

In this paper, we aim to improve the performance of DOA estimation under the premise of eliminating acoustic velocity. Then, an arbitrary cross-linear nested array is designed while the CRB of the arrays used by the previous algorithms are analyzed. The theoretical performance of the cross-linear nested array is better than that of the uniform array, despite it is still inferior the linear nested array. Hence, a TVI-ESPRIT algorithm via the cross-linear nested array is presented to optimize the method with the unknown velocity. It has the advantages of the flexible array arrangement, eliminating acoustic velocity error and relatively high DOA estimation accuracy. Simulation results demonstrate the effectiveness of the algorithm and its unique advantages.

The notations $(\cdot)^*$, $(\cdot)^T$, $(\cdot)^H$, $(\cdot)^{-1}$ and $(\cdot)^\dagger$ donate conjugation, transposition, conjugate-transposition, inverse, and pseudo-inversion, respectively. $E(\cdot)$ indicates the operation of expectation. arg$(\cdot)$ means the phase angle of complex number. diag$(\cdot)$ represents the diagonalization operator. The scalar is denoted by x, vector by $\boldsymbol{x}$, and matrix by $\boldsymbol{X}$.

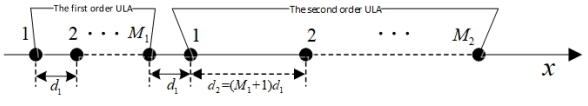

Figure 1: Nested linear Array Structure

2 Data model of the nested array

It is assumed that K far-field narrowband acoustic signals impinge on a nested linear array with M sensors in the underwater channel. Considering that each sensor collects N time snapshots, the signal observations

matrix $\boldsymbol{X} \in \mathbb{C}^{M\times N}$ of nested linear array can be expressed as

$$\boldsymbol{X} = \boldsymbol{A}(\boldsymbol{\theta})\boldsymbol{S} + \boldsymbol{N} \tag{1}$$

where $\boldsymbol{A}(\boldsymbol{\theta}) = [\boldsymbol{a}(\theta_1), \ldots, \boldsymbol{a}(\theta_K)] \in \mathbb{C}^{M\times K}$ is the array steering matrix, which consists of the array steering vectors $\boldsymbol{a}(\theta_k), k = 1, \ldots, K$. And $\boldsymbol{S} \in \mathbb{C}^{K\times N}$ is the sampling matrix of the time domain signals. In addition, $\boldsymbol{N} \in \mathbb{C}^{M\times N}$ is the additive noise matrix of the array, and Gaussian White Noise is generally used.

The nested array usually refers to the combined array composed of two uniform linear arrays. The two linear arrays are connected in series to form the nested linear array we use, as shown in Figure 1. The number of elements in the first-order uniform linear array is M_1, and the interval between sensors is d_1(Usually the half of the signal wavelength). And the number of elements in the second-order uniform linear array is M_2, and the interval between sensors is $d_2 = (M_1+1)\times d_1$. Therefore, the sensor layout set D of the linear nested array is

$$\begin{cases} D_1 &= \{m_1 d_1, m_1 = 1, 2, \ldots, M_1\} \\ D_2 &= \{m_2(M_1+1)d_1, m_2 = 1, 2, \ldots, M_2\} \\ D &= D_1 \cup D_2 \end{cases} \tag{2}$$

Then, the covariance matrix $\boldsymbol{R}_x$ of the linear nested array can be expressed as

$$\begin{aligned} \boldsymbol{R}_x &= E[\boldsymbol{X}\boldsymbol{X}^H] \\ &= \boldsymbol{A}(\boldsymbol{\theta})\boldsymbol{R}_s\boldsymbol{A}^H(\boldsymbol{\theta}) + \sigma_n^2\boldsymbol{I} \end{aligned} \tag{3}$$

where $\boldsymbol{R}_s \in \mathbb{C}^{K\times K}$ is the correlation matrix of the signal. And σ_n^2 is the power of Gaussian white noise, $\boldsymbol{I} \in \mathbb{C}^{M\times M}$. Then, the data covariance matrix $\boldsymbol{R}_x$ is transformed into vector

$$\begin{aligned} \boldsymbol{z} = \mathrm{vec}\{\boldsymbol{R}_x\} &= (\boldsymbol{A}^* \otimes \boldsymbol{A})\mathrm{vec}\{\boldsymbol{R}_s\} + \sigma_n^2\mathrm{vec}\{\boldsymbol{I}\} \\ &= (\boldsymbol{A}^* \odot \boldsymbol{A})\boldsymbol{p} + \sigma_n^2\boldsymbol{I}_n \end{aligned} \tag{4}$$

In the above Equation, $\odot$ represents the Khatri-Rao product, and $\otimes$ represents the Kronecker product. $\boldsymbol{p} = [\sigma_1^2, \sigma_2^2, \ldots, \sigma_K^2]^T \in \mathbb{C}^{K\times 1}$ represents the power vector of the signals. $\boldsymbol{I}_n$ is the vectorized identity matrix. Therefore, the vectorization transformation in the above Equation must assume that the signals are independent from each other, especially the step of the transition to the Khatri-Rao product.

So here we have a new steering matrix $\boldsymbol{B} = \boldsymbol{A}^* \odot \boldsymbol{A}$ while $\boldsymbol{z}$ can be thought as a single snapshot array signal vector. In this case, the signal receiving model can be regarded as the signal received by the extended uniform linear array. However, it is out of order and has some redundancy. We need to reorder it and get rid of the redundancy. Then a new equivalent signal vector

$$\bar{\boldsymbol{z}} = \boldsymbol{A}_r\boldsymbol{p} + \sigma_n^2\boldsymbol{I}_n \tag{5}$$

is obtained. Assume that the number of equivalent elements after the array extension is M_{ex}. Then $\boldsymbol{A}_r \in \mathbb{C}^{M_{ex}\times K}$ is its steering matrix. In general, in order to obtain the maximum extended aperture (or degree of freedom) of the array, we often set up nested arrays according to the following criteria:

$$\begin{cases} M_1 = M_2 = \frac{M}{2} & M\text{is an even number} \\ M_1 = \frac{M-1}{2}, M_2 = \frac{M+1}{2} & M\text{is an odd number} \end{cases} \tag{6}$$

Since the equivalent signal has only one snapshot, we need to restore the rank of the equivalent data covariance matrix by constructing Toeplitz matrix $\boldsymbol{R}_{tp}$. Suppose the aperture of array are M_{tp}.

$$\boldsymbol{R}_{tp} = \begin{bmatrix} \bar{\boldsymbol{z}}_{M_{tp}} & \bar{\boldsymbol{z}}_{M_{tp}-1} & \cdots & \bar{\boldsymbol{z}}_1 \\ \bar{\boldsymbol{z}}_{M_{tp}+1} & \bar{\boldsymbol{z}}_{M_{tp}} & \cdots & \bar{\boldsymbol{z}}_2 \\ \vdots & \vdots & \ddots & \vdots \\ \bar{\boldsymbol{z}}_{2M_{tp}-1} & \bar{\boldsymbol{z}}_{2M_{tp}-2} & \cdots & \bar{\boldsymbol{z}}_{M_{tp}} \end{bmatrix} \tag{7}$$

Here we review the traditional ESPRIT algorithm using $\boldsymbol{R}_{tp}$ as an example. First, the eigenvalue decomposition of the matrix $\boldsymbol{R}_{tp}$ is carried out, and we can obtain the signal subspace spanned by K larger eigenvalues corresponding eigenvectors $\boldsymbol{U}_s \in \mathbb{C}^{M_{tp}\times K}$. Then the signal subspace is divided into the signal subspace ($\boldsymbol{U}_{s1} \in \mathbb{C}^{(M_{tp}-1)\times K}$ and $\boldsymbol{U}_{s2} \in \mathbb{C}^{(M_{tp}-1)\times K}$) of two subarrays respectively.

$$\begin{cases} \boldsymbol{U}_{s1} = \boldsymbol{U}_s(1 : M_{tp}-1, :) \\ \boldsymbol{U}_{s2} = \boldsymbol{U}_s(2 : M_{tp}, :) \end{cases} \tag{8}$$

Their corresponding steering matrices can be expressed as

$$\begin{cases} \boldsymbol{A}_{r1} = \boldsymbol{A}_r(1 : M_{tp}-1, :) \\ \boldsymbol{A}_{r2} = \boldsymbol{A}_r(2 : M_{tp}, :) \end{cases} \tag{9}$$

There is a rotation matrix $\boldsymbol{\Phi}$ relationship between the steering vectors of the two submatrices because of the unit space ($\Delta = d_1$) between the two subarrays.

$$\boldsymbol{\Phi} = \mathrm{diag}\{\mathrm{e}^{j\frac{2\pi\Delta\sin\theta_1}{\lambda}}, \mathrm{e}^{j\frac{2\pi\Delta\sin\theta_2}{\lambda}}, \ldots, \mathrm{e}^{j\frac{2\pi\Delta\sin\theta_K}{\lambda}}\} \tag{10}$$

In addition, due to the correspondence between the signal subspace $\boldsymbol{U}_s$ and the steering matrix $\boldsymbol{A}_r$, there must be a non-singular unitary matrix $\boldsymbol{T} \in \mathbb{C}^{K\times K}$, which satisfies the following relation:

$$\begin{bmatrix}\boldsymbol{U}_{s1}\\ \boldsymbol{U}_{s2}\end{bmatrix} = \begin{bmatrix}\boldsymbol{A}_{r1}\boldsymbol{T}\\ \boldsymbol{A}_{r1}\boldsymbol{\Phi}\boldsymbol{T}\end{bmatrix} \tag{11}$$

Further, we can get the following result:

$$\boldsymbol{\Psi} = \boldsymbol{U}_{s1}^{\dagger}\boldsymbol{U}_{s2} = \boldsymbol{T}^{-1}\boldsymbol{\Phi}\boldsymbol{T} \tag{12}$$

By using the property that the diagonal elements of matrix $\boldsymbol{\Phi}$ are equal to the eigenvalues of matrix $\boldsymbol{\Psi}$, the diagonal elements of matrix $\boldsymbol{\Phi}$ can be estimated. And the arrival angle of the signal can be obtained, too.

3 Velocity-independent method based on the arbitrary cross-linear nested array

In this section, we propose a DOA estimation method to eliminate the underwater acoustic velocity error. We use a cross-linear nested array, as shown in Figure 2.

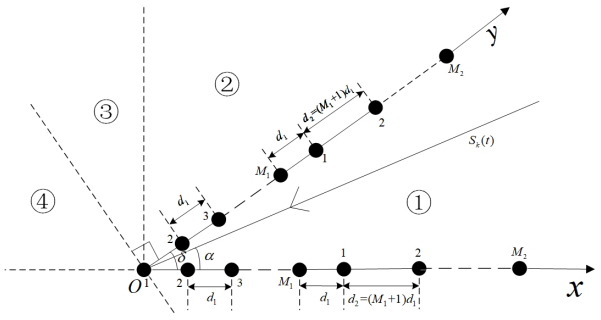

Figure 2: Arbitrary Cross-linear Nested linear Array Structure

We take the sensor at the intersection of two linear arrays as the reference array element. Assuming that the cross angle between two linear arrays is δ, we divide the one-dimensional space into four parts by taking the axes where the two linear arrays are located and their normal lines as the boundary. Suppose that the coordinate axes of the two linear arrays are respectively X-axis and Y-axis, and the angle between the incoming direction of the kth signal ($k = 1, 2, \ldots, K$) and the X-axis normal is x_{nk}, and the angle between the incoming direction and the Y-axis normal is y_{nk}. The angle between the wave arrival direction and the X-axis is α, through the classification discussion, we derive the following relationship:

$$\begin{cases} x_{nk} + y_{nk} = \pi - \delta & \text{DOA in the area 1}\\ y_{nk} - x_{nk} = \delta & \text{DOA in the area 2}\\ x_{nk} + y_{nk} = \delta & \text{DOA in the area 3}\\ x_{nk} - y_{nk} = \delta & \text{DOA in the area 4}\end{cases} \tag{13}$$

Then, the sensor at the intersection is also taken as the reference element. When the incident signal reaches the reference element first, the incoming direction of the X-axis or Y-axis (θ_{xk}, θ_{yk}) is positive. Otherwise, when the incident signal reaches the reference element last, the direction of incoming wave (θ_{xk}, θ_{yk}) is negative. After analyzing, the following relationship is obtained.

$$\begin{cases} \theta_{xk} = -x_{nk}, \quad \theta_{yk} = -y_{nk} & \text{DOA in the area 1}\\ \theta_{xk} = -x_{nk}, \quad \theta_{yk} = -y_{nk} & \text{DOA in the area 2}\\ \theta_{xk} = +x_{nk}, \quad \theta_{yk} = -y_{nk} & \text{DOA in the area 3}\\ \theta_{xk} = +x_{nk}, \quad \theta_{yk} = +y_{nk} & \text{DOA in the area 4}\end{cases} \tag{14}$$

Substituting Equation (14) back to Equation (13) in turn, we can conclude that the relation between the arrival angles of the same signal to two linear-arrays is

$$\sin\theta_{yk} = \sin(\theta_{xk} - \delta) \quad k = 1, 2, \ldots, K \tag{15}$$

Following Equation (12), we performed ESPRIT algorithm on the X-line array and the Y-line array to obtain their respective rotation matrices: $\boldsymbol{\Phi}_X$ and $\boldsymbol{\Phi}_Y$, respectively. Then, we list the rotational phase of the two axes separately, for the kth signal ($k = 1, 2, \ldots, K$),

$$\begin{cases} \arg(\hat{\Phi}_{xk}) = \frac{2\pi f \Delta \sin\hat{\theta}_{xk}}{c_k}\\ \arg(\hat{\Phi}_{yk}) = \frac{2\pi f \Delta \sin\hat{\theta}_{yk}}{c_k}\end{cases} \tag{16}$$

By Equation (16), we get

$$\frac{\arg(\hat{\Phi}_{yk})}{\arg(\hat{\Phi}_{xk})} = \frac{\sin\hat{\theta}_{yk}}{\sin\hat{\theta}_{xk}} \tag{17}$$

From such a process, it is clear that the acoustic velocity is eliminated by reduction of the fraction. Thus, it eliminates the error caused by acoustic velocity in DOA estimation at the same time. Next, we need to substitute Equation (15) into Equation (17), and then the kth DOA value is estimated (We take the X-axis as the main axis).

$$\hat{\theta}_k = \operatorname{arccot}(\cot\delta - \frac{\arg(\hat{\Phi}_{yk})}{\arg(\hat{\Phi}_{xk})\sin\delta}) \tag{18}$$

For a single signal, the algorithm has completed DOA estimation. However, in the case of multiple signals in the channel, we need to add some conditions to Equation (17) to complete their pairing. For the receiver sensors, the acoustic velocity received by each of them is similar (from $1450m/s$ to $1550m/s$). After deducting the Equation (16), we can get the calculation expression of the kth acoustic signal velocity as

$$\hat{c}_k = \frac{2\pi\Delta f \sin\delta}{\sqrt{\arg^2(\hat{\Phi}_{xk}) + \arg^2(\hat{\Phi}_{yk}) - 2\arg(\hat{\Phi}_{xk})\arg(\hat{\Phi}_{yk})\cos\delta}} \tag{19}$$

Then, we can list all the paired combinations of $\{\arg(\hat{\Phi}_{yk})\}$ and $\{\arg(\hat{\Phi}_{xk})\}$, there are $K!$ kinds of combinations in total. For each combination, Equation (19) can be used to find the acoustic velocities $\{\hat{c}_k, k = 1, 2, \ldots, K\}$ of K signals. Finally, we can find the group with the smallest variance of acoustic velocity estimation, which corresponds to the correct pair combination.

$$\min_i \operatorname{var}(\{\hat{c}_k\}_i), \quad i = 1, 2, \ldots, K! \tag{20}$$

As the proposed acoustic velocity independent algorithm uses Toeplitz matrix reconstruction technology, it is named TVI-ESPRIT algorithm.

4 CRB analysis on the proposed algorithm

Before the simulation experiment, the Cramer-Rao bound (CRB) analysis on this parameter estimation problem should be done. The parameter vectors to be estimated are denoted as $\boldsymbol{\Theta} = [\theta_1, \theta_2, \ldots, \theta_K]^T$. Since the data vector received by the array can be considered as a general Gaussian process, i.e

$$\boldsymbol{x}(n) \sim \mathcal{N}(\sum_{k=1}^{K} \boldsymbol{a}(\theta_k)\boldsymbol{s}_k(n), \boldsymbol{C}) \tag{21}$$

Here, $\boldsymbol{C}$ is the covariance matrix of the receiving vector in the nth moment $\boldsymbol{x}(n)$. The data received by each sensor are irrelevant, so $\boldsymbol{C} = \sigma_n^2 \boldsymbol{I}_M$.

In addition, the algorithm proposed in this paper is based on arbitrary cross-linear nested array and its direction vector is denoted as

$$\begin{aligned}\boldsymbol{a}(\theta_k) = [&e^{-j\omega\tau_{k1}}, \ldots, e^{-j\omega\tau_k\frac{M+1}{2}}, \\ &e^{-j\omega\tau_k\frac{M+3}{2}}, \ldots, e^{-j\omega\tau_{kM}}]^T\end{aligned} \tag{22}$$

$$\tau_{km} = \begin{cases} \frac{x_m \sin\theta_k}{c} & m \in [1, \frac{M+1}{2}] \\ \frac{y_{m-\frac{M+1}{2}} \sin(\theta_k - \delta)}{c} & m \in [\frac{M+3}{2}, M] \end{cases} \tag{23}$$

, where τ_{km} is the time delay between sensors, and $\{x_m\}$ and $\{y_m\}$ are the location set of two linear array sensors respectively. The number of sensors M is odd.

Through the reference [22], the Fisher information matrix $\boldsymbol{I}(\boldsymbol{\Theta})$ of the General Gaussian process is derived. And the i, jth element of $\boldsymbol{I}(\boldsymbol{\Theta})$ is

$$\begin{aligned}[\boldsymbol{I}(\boldsymbol{\Theta})]_{i,j} &= [\frac{\partial\boldsymbol{\mu}(\boldsymbol{\Theta})}{\partial\theta_i}]^H \boldsymbol{C}^{-1}(\boldsymbol{\Theta})[\frac{\partial\boldsymbol{\mu}(\boldsymbol{\Theta})}{\partial\theta_j}] + \frac{1}{2}tr[\boldsymbol{C}^{-1}(\boldsymbol{\Theta})\frac{\partial\boldsymbol{C}(\boldsymbol{\Theta})}{\partial\theta_i}\boldsymbol{C}^{-1}(\boldsymbol{\Theta})\frac{\partial\boldsymbol{C}(\boldsymbol{\Theta})}{\partial\theta_j}] \\ &= \frac{\boldsymbol{s}_i^H\boldsymbol{s}_j\omega^2}{\sigma_n^2 c^2}\{\cos\theta_i\cos\theta_j \sum_{m=1}^{\frac{M+1}{2}}[x_m^2 e^{\frac{j\omega x_m(\sin\theta_i - \sin\theta_j)}{c}}] \\ &+ \cos(\theta_i - \delta)\cos(\theta_j - \delta) \sum_{m=\frac{M+3}{2}}^{M}[y_{m-\frac{M+1}{2}}^2 e^{\frac{j\omega x_m(\sin(\theta_i-\delta) - \sin(\theta_j-\delta))}{c}}]\}\end{aligned} \tag{24}$$

When $i = j$,

$$[\boldsymbol{I}(\boldsymbol{\Theta})]_{i,i} = \frac{2N\omega^2\mathrm{snr}}{c^2}[\cos^2\theta_i \sum_{m=1}^{\frac{M+1}{2}} x_m^2 + \cos^2(\theta_i - \delta) \sum_{m=\frac{M+3}{2}}^{M} y_{m-\frac{M+1}{2}}^2] \tag{25}$$

Here, $\mathrm{snr} = \frac{E[\boldsymbol{s}_i^*(n)\boldsymbol{s}_i(n)]}{2\sigma_n^2}$, $\boldsymbol{s}_i^H\boldsymbol{s}_j = N * E[\boldsymbol{s}_i^*(n)\boldsymbol{s}_j(n)]$. It is assumed that the signals are irrelevant, so the following data relationship holds

$$E[\boldsymbol{s}_i^*(n)\boldsymbol{s}_i(n)] \gg E[\boldsymbol{s}_i^*(n)\boldsymbol{s}_j(n)] \approx 0 \tag{26}$$

Then, the Fisher information matrix $\boldsymbol{I}(\boldsymbol{\Theta})$ of DOA estimation in our proposed algorithm is

$$\boldsymbol{I}(\boldsymbol{\Theta}) = \mathrm{diag}\{[\boldsymbol{I}(\boldsymbol{\Theta})]_{1,1}, [\boldsymbol{I}(\boldsymbol{\Theta})]_{2,2}, \ldots, [\boldsymbol{I}(\boldsymbol{\Theta})]_{K,K}\} \tag{27}$$

where $diag\{\cdot\}$ means the diagonal matrix formed with the contained elements. we can obtain the CRB of the kth DOA.

$$\mathrm{CRB}(\theta_k) = \sqrt{[\boldsymbol{I}(\boldsymbol{\Theta})]^{-1}_{k,k}} = \sqrt{\frac{c^2}{2\omega^2 N \mathrm{snr}} \frac{1}{\cos^2\theta_k \sum_{m=1}^{\frac{M+1}{2}} x_m^2 + \cos^2(\theta_k - \delta) \sum_{m=\frac{M+3}{2}}^{M} y^2_{m-\frac{M+1}{2}}}} \tag{28}$$

And the total CRB of 1D DOAs can be expressed by the following equation.

$$\mathrm{CRB} = \sqrt{\frac{1}{K}\sum_{k=1}^{K}[\boldsymbol{I}(\boldsymbol{\Theta})]^{-1}_{k,k}} \tag{29}$$

According to Equation (28) and (29), it can be concluded that the CRB of 1D DOAs decreases as the number of snapshots or SNR increases. And the array structure also has an impact on the CRB, including the number and location of sensors. Especially, when the cross-linear angle δ of the proposed structure is equal to the incoming direction, the CRB of DOA estimation can be optimized for the structure. The following simulation experiments also verify these conclusions.

Now a summary of the proposed algorithm is made in the Table 1 below.

Table 1: The Flow Scheme of TVI-ESPRIT Algorithm

Input:

A cross-linear nested array with M sensors at a cross angle of δ;

The receiving matrix of array signals with N snapshots in the time domain, $\boldsymbol{X} \in \mathbb{C}^{M\times N}$;

Output:

1: Calculate and vectorize the signal covariance matrices ($\boldsymbol{R}_x$ and $\boldsymbol{R}_y$) of two nested line arrays by Equation (3) and (4) respectively. $\boldsymbol{z}_x$ and $\boldsymbol{z}_y$ can be obtained;
2: Reorder them and get rid of the redundancy and obtain $\bar{z}_x$ and $\bar{z}_y$ as the Equation (5);
3: Construct the Toeplitz matrices applicable to the two axes respectively by the Equation (7);
4: Utilize LS-ESPRIT algorithm to calculate the matrices Ψ_x and Ψ_y of two linear-arrays by Equation (8) and (12), respectively;
5: By the eigenvalue decomposition of the matrices Ψ_x and Ψ_y, the values of the rotation matrices $\hat{\boldsymbol{\Phi}}_x$ and $\hat{\boldsymbol{\Phi}}_y$ of two linear-arrays can be estimated respectively;
6: Complete the pairing between the diagonal elements of the two rotation matrices by the criterion of Equation (20);
7: Complete the final DOA estimation by the Equation (18);
8: **return** DOAs: $\hat{\boldsymbol{\theta}}$.

5 Simulation results and discussion

In this section, we evaluate the performance of the proposed TVI-ESPRIT algorithm and compare it with the other ESPRIT algorithms. These algorithms include TLS-ESPRIT [7], MS-KAI-ESPRIT [9], GLS-ESPRIT [10] algorithm based on a uniform linear array, SS-ESPRIT [23] algorithm based on a nested linear array and VI-ESPRIT [20] algorithm based on L-shaped uniform linear array. To be fair, the array used by all the algorithms includes $M = 11$ sensors, and the cross angle of the cross-linear nested array is $\delta = 45°$.

Unless otherwise specified, all simulation results are obtained for the case of sources with $f = 10Hz$ center frequency by means of $W = 1000$ Monte Carlo trials with $f_s = 20Hz$ sampling frequency and $N = 200$ snapshots. Nextly, the SNR of the signal is set to $0dB$ in Additive White Gaussian Noise situation, and the incoming direction of the single signal is $\theta = 30°$.

The expected acoustic velocity is set to $1500m/s$. The unit spacing between the sensors is half of the expected acoustic wavelength. Note that $\Delta c = c_{real} - c_0$, where $c_0 = 1500m/s$.

After practical deducting, the theoretical expression of the error caused by acoustic velocity error is

$$Error_c = |\theta - \arcsin(\frac{c_0 \sin\theta}{c_{real}})| \tag{30}$$

where c_{real} represents the actual acoustic velocity. $Error_c$ will be used as the reference of simulation experiment to reflect the influence of acoustic velocity error on estimation accuracy.

5.1 Effect of array structure on estimation performance

In the first experiment, the simulation of the array structures utilized by the algorithms is done. Four kinds of structures are compared in terms of CRB in total.

Figure 3 (a) and (b) show that the cross-linear nested array is superior to the uniform linear array and the L-shaped uniform linear array, but it is inferior to the nested linear array when given the same number of sensors. This is because in the array used in the proposed algorithm, half of the sensors are used to eliminate the acoustic velocity factor, thus affecting the estimation performance. However, due to the expanded aperture of the nested array, it can make up for the lack of algorithmic precision to some extent.

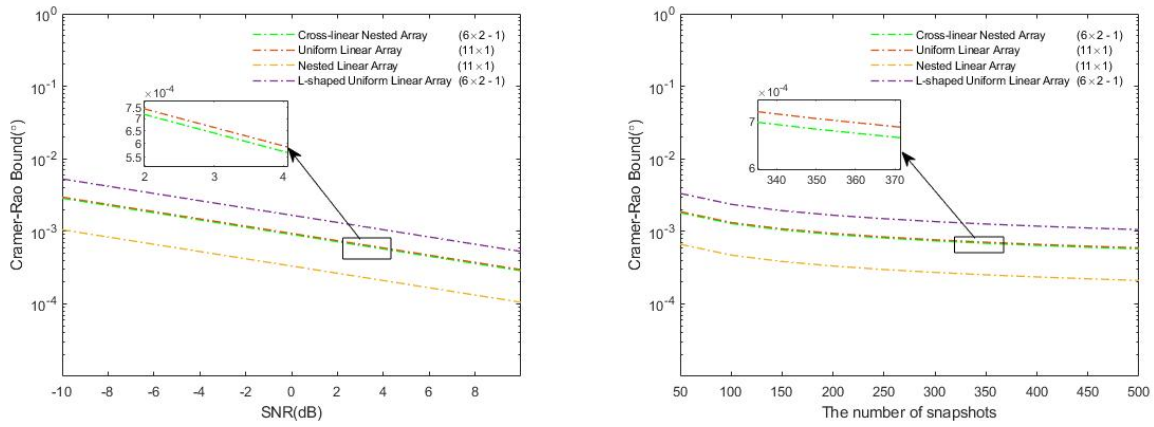

(a) (b)

Figure 3: (**a**) CRB versus structures and SNR with $c = 1500m/s, f = 10kHz, \theta = 30°, N = 200$; (**b**) CRB versus structures and the number of snapshots with $c = 1500m/s, f = 10kHz, \theta = 30°, SNR = 0dB$.

5.2 Effect of cross-linear angle on estimation performance

In the second experiment, all algorithms are compared in terms of RMSE over cross angle δ. A far-field narrowband signal with a center frequency of $10kHz$ arrives the sensor array. Then, we set the angle of arrival to 60°. We have done $W = 1000$ Monte Carlo simulations and calculated their root mean square error ($RMSE$) to measure the accuracy of the estimation. RMSE is defined as followed:

$$RMSE = \sqrt{\frac{1}{WK}\sum_{k=1}^{K}\sum_{w=1}^{W}(\hat{\theta}_{k,w} - \theta_k)^2} \tag{31}$$

Based on the above result in Figure 4, we find that the estimation performance of DOA is optimal when the cross-linear angle and arrival angle are equal, which is consistent with the CRB analysis. In practice, the real direction of arrival is unmeasured and unknown, and we cannot optimize the cross-linear angle. When the incoming wave direction is from 0° to 90°, it is relatively appropriate to set the cross angle as 45°.

5.3 Effect of incoming direction on estimation performance

In the third experiment, all algorithms are also compared in terms of RMSE over wave directions. Each case with an incoming wave direction θ in the range 10° to 80° is tested. Simulation experiments are carried out in the environment where the acoustic velocity errors Δc are $0m/s$ and $20m/s$ respectively.

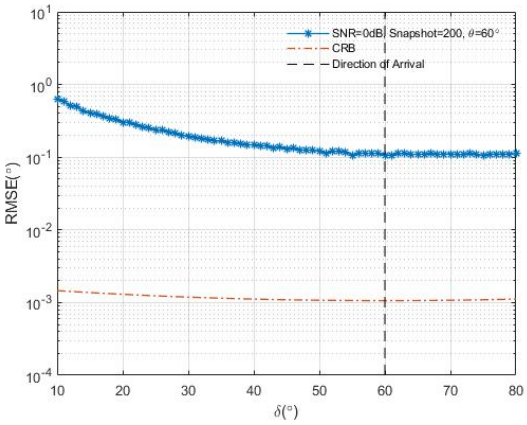

Figure 4: RMSE versus cross-linear angles $\Delta c = 20m/s, \theta = 60°, SNR = 0dB, N = 200$

It can be seen from the Figure 5 (a) and (b) that when the direction of the incoming wave approaches 90°, the error of estimation increases obviously. The proposed algorithm is actually more accurate than the traditional acoustic velocity independent algorithms. The other ESPRIT algorithms are obviously affected by the acoustic velocity error. The principal factor of the error is from the acoustic velocity error even, because their $RMSE$ curves almost coincide with $Error_c$ curve. While, our TVI-ESPRIT algorithm is not affected by the acoustic velocity error and its performance is far better than that of VI-ESPRIT algorithm. Finally, although the proposed algorithm is not

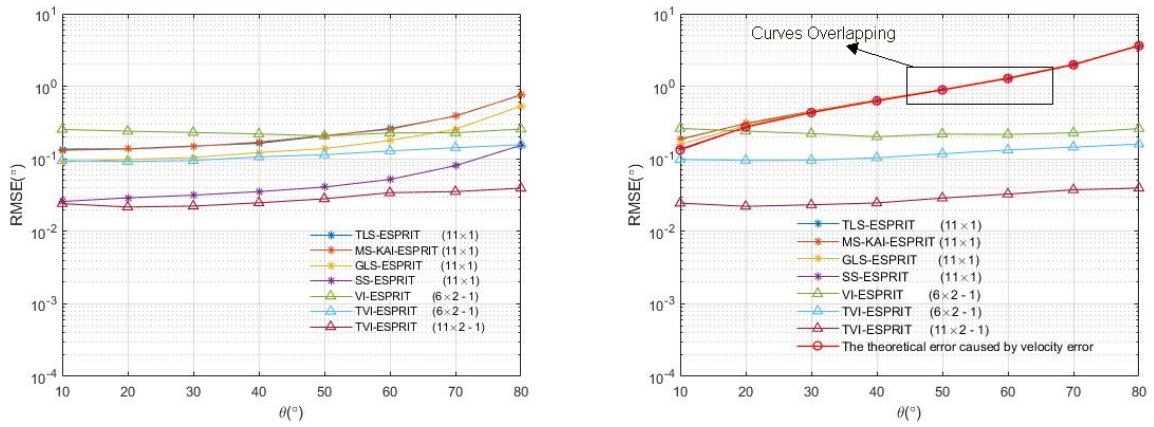

(a) (b)

Figure 5: RMSE versus directions of arrival (**a**) $\Delta c = 0m/s, SNR = 0dB, N = 200$; and (**b**) $\Delta c = 20m/s, SNR = 0dB, N = 200$.

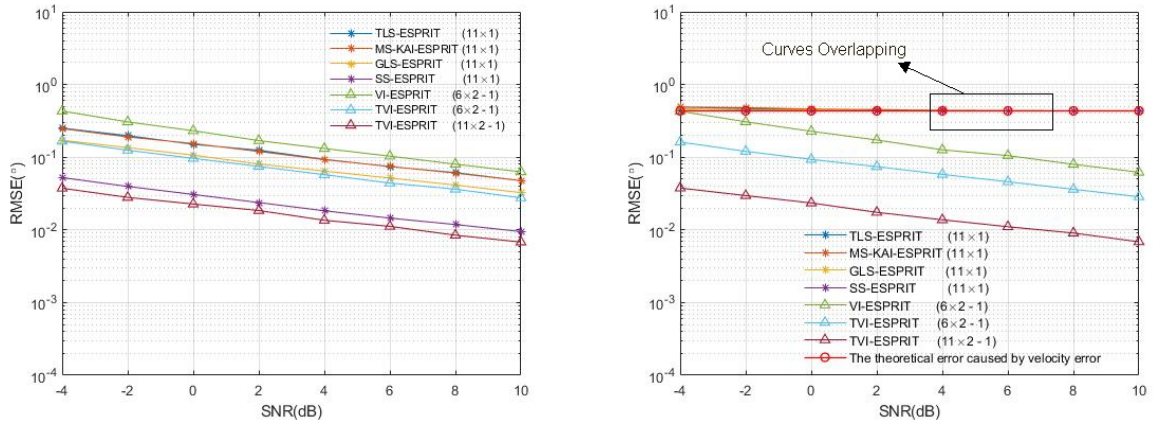

(a) (b)

Figure 6: RMSE under different SNR condition (**a**) $\Delta c = 0m/s, N = 200, \theta = 30°$; and (**b**) $\Delta c = 20m/s, N = 200, \theta = 30°$.

as good as SS-ESPRIT algorithm in the environment without acoustic velocity error, it still maintains good estimation accuracy.

5.4 Comparison of algorithms with different SNR

In the fourth simulation experiment, we have compared the other algorithms with the TVI-ESPRIT algorithm under different SNR conditions. Just like the previous experiment, we also set the acoustic velocity error as $0m/s$ and $20m/s$, and conducted $W = 1000$ Monte Carlo simulation experiments with the direction of arrival 30° under each SNR condition.

As can be seen from the Figure 6 (a), TVI-ESPRIT is inferior to SS-ESPRIT in estimation accuracy without acoustic velocity error, but it still maintains good performance compared with the other algorithms. According to the results in Figure 6 (b), all ESPRIT algorithms via a single linear array are inevitably caused by systematic errors of inaccurate acoustic velocity, no matter how large the SNR value is. In addition, the algorithm proposed in this paper greatly improves the estimation accuracy compared with the traditional VI-ESPRIT algorithm.

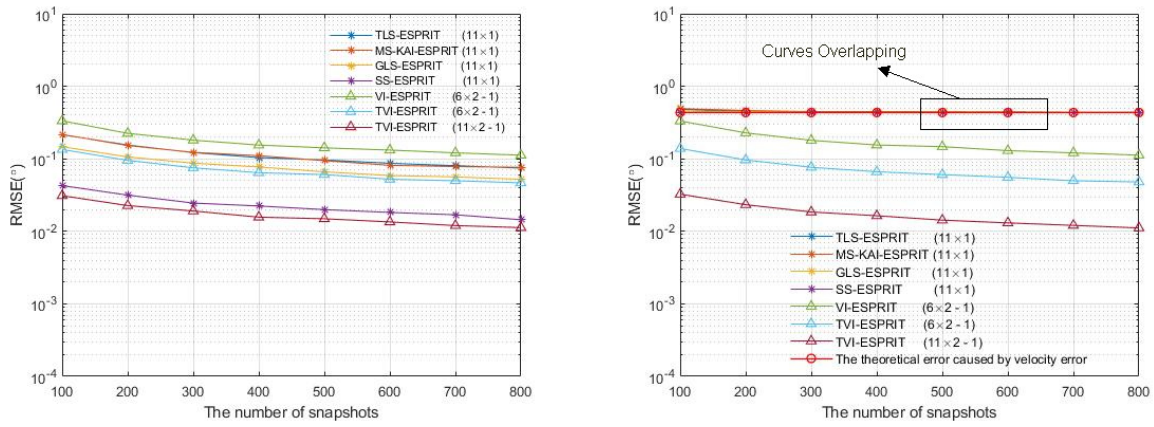

(a) (b)

Figure 7: RMSE under different number of snapshots (**a**) $\Delta c = 0m/s, SNR = 0dB, \theta = 30°$; and (**b**) $\Delta c = 20m/s, SNR = 0dB, \theta = 30°$.

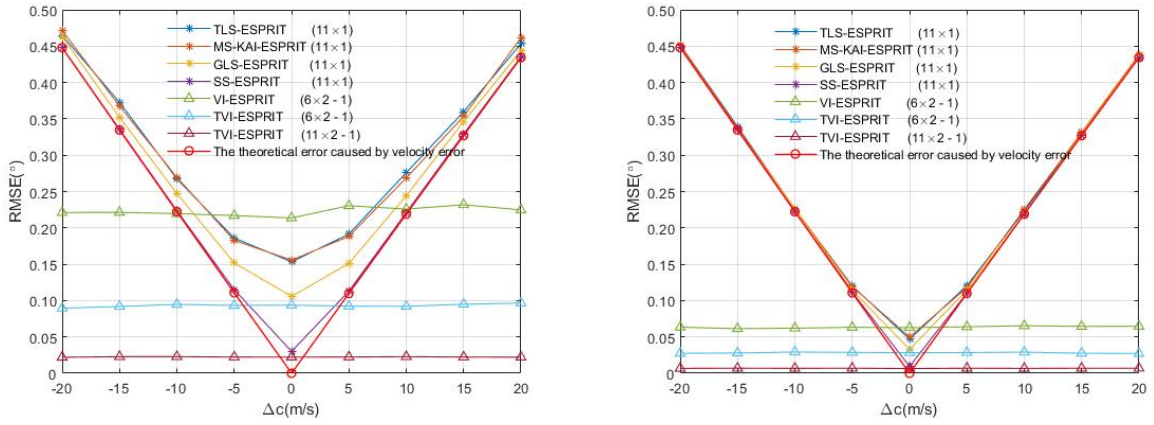

(a) (b)

Figure 8: RMSE under different acoustic velocity (**a**) $N = 200, SNR = 0dB, \theta = 30°$; and (**b**) $N = 200, SNR = 10dB, \theta = 30°$.

5.5 Comparison of algorithms with different number of snapshots

In the fifth simulation experiment, the above algorithms are compared in terms of RMSE with respect to the number of sampling snapshots. The condition of the simulation is the same as the overall setting.

Figure 7 (a) shows that TVI-ESPRIT algorithm is better than other ESPRIT algorithms even though its performance is not as good as SS-ESPRIT algorithm without acoustic velocity error. And in Figure 7 (b), ESPRIT algorithms via a single linear array are generally greatly affected by acoustic velocity error, and their main factor of error is inaccurate acoustic velocity, no matter how large their numbers of snapshots are. In addition, the estimation accuracy of the proposed algorithm is generally better than that of VI-ESPRIT algorithm. The conclusion of this experiment is similar to that of the previous experiment.

5.6 Comparison of algorithms with unknown acoustic velocity

In the last experiment, the above algorithms are compared in terms of RMSE with respect to specific acoustic velocity error. The other simulation experiment parameters are the same as those of the overall setting.

From the two result figures (Figure 8 (a) and (b)), the estimation error of the ESPRIT algorithms based on a single linear array increase as the absolute value of the acoustic velocity error increases. Meanwhile, the estimation accuracy of the two VI algorithms are almost not affected by the acoustic velocity error. In addition, TVI-ESPRIT algorithm is better than the traditional VI-ESPRIT algorithm on the aspect of estimation accuracy, especially in the case of low SNR condition. Nextly, in the case of low SNR, the estimation error of traditional ESPRIT algorithms based on linear-array mainly come from noise and acoustic velocity. While at high SNR condition, their estimation error mainly comes from acoustic velocity. This can be reflected from the fact that with the increasement of SNR, their RMSE curves keep approaching the Error_c curve caused by the theoretical error due to the acoustic velocity error. Finally, our TVI-ESPRIT is slightly inferior to SS-ESPRIT without acoustic velocity error, but it is still superior to the other ESPRIT algorithms.

6 CONCLUSIONS

In order to eliminate the influence of underwater acoustic velocity on DOA estimation accuracy, we propose a TVI-ESPRIT algorithm using an arbitrary cross-linear nested array. The proposed method employs the rotational phase matrix of two crossed linear arrays to eliminate the acoustic velocity factor, but the traditional ESPRIT algorithm (GLS-ESPRIT, etc.) based on linear array can't. In addition, it expands the aperture of the array on the algorithm level, so its estimation accuracy is higher than that of the former VI-ESPRIT algorithm. Simulation results verified the validity of the above conclusions.

Abbreviations

TLS-ESPRIT: Total Least Square Estimating Signal Parameter via Rotational Invariance Techniques
MS-KAI-ESPRIT: Multistep Knowledge-Aided Iterative Estimating Signal Parameter via Rotational Invariance Techniques
GLS-ESPRIT: Generalized Least Square Estimating Signal Parameter via Rotational Invariance Techniques
SS-ESPRIT: Estimating Signal Parameter via Rotational Invariance Techniques using spatial smoothing technique
VI-ESPRIT: Velocity Independent Estimating Signal Parameter via Rotational Invariance Techniques
TVI-ESPRIT: Velocity Independent Estimating Signal Parameter via Rotational Invariance Techniques using Toeplitz matrix reconstruction

Acknowledgements

The authors would like to thank all anonymous reviewers and editors for their helpful suggestions for the improvement of this paper.

Author's contributions

GN and GJ proposed the original idea of the full text; GN and YW designed and implemented the simulation experiments; YW and XZ wrote the manuscript under the guidance of GN. All authors read and approved this submission.

Funding

This work was supported by the National Natural Science Foundation of China (61871191), and the Science Technology Planning Project of Guangzhou (202002030251), and the Natural Science Foundation of Guangdong Province (2020A1515010962).

Competing interests

The authors declare that they have no competing interests.

Author details

[1] South China University of Technology, Guangzhou, China. [2] Guangdong University of Technology, Guangzhou, China.

References

1. Shi, J., Hu, G., Zhang, X., Sun, F., Zheng, W., Xiao, Y.: Generalized co-prime mimo radar for doa estimation with enhanced degrees of freedom[J]. IEEE Sensors Journal **18**(3), 1203–1212 (2017)
2. Sun, M., Pan, J., Bastard, C.L., Wang, Y., Li, J.: Advanced signal processing methods for ground-penetrating radar: Applications to civil engineering[J]. IEEE Signal Processing Magazine **36**(4), 74–84 (2019)
3. Dong, F., Jiang, Y., Yan, Y., Yang, Q., Xie, X.: Direction-of-arrival tracking using a co-prime microphone array: A particle filter perspective[J]. Applied Acoustics **170**, 107499 (2020)
4. Li, J.: Doa tracking in time-varying underwater acoustic communication channels[C]. In: Oceans (2017)
5. Jian, C., Shen, Z., Huang, Z., Qiao, C.: Acoustic velocity measurement in seawater based on phase difference of signal[C]. In: International Conference on Electronic Measurement & Instruments (2011)
6. Schmidt, R.: Multiple emitter location and signal parameter estimation[J]. IEEE transactions on antennas and propagation **34**(3), 276–280 (1986)
7. Roy, R., Kailath, T.: Esprit-estimation of signal parameters via rotational invariance techniques[J]. IEEE Transactions on acoustics, speech, and signal processing **37**(7), 984–995 (1989)
8. Xudong, W., Zhang, X., Li, J., Bai, J.: Improved esprit method for joint direction-of-arrival and frequency estimation using multiple-delay output[J]. International Journal of Antennas and Propagation **2012** (2012)
9. Pinto, S.F., De Lamare, R.C.: Multistep knowledge-aided iterative esprit: design and analysis[J]. IEEE Transactions on Aerospace and Electronic Systems **54**(5), 2189–2201 (2018)
10. Steinwandt, J., Roemer, F., Haardt, M.: Generalized least squares for esprit-type direction of arrival estimation[J]. IEEE Signal Processing Letters **24**(11), 1681–1685 (2017)
11. Esfandiari, M., Vorobyov, S.A.: Enhanced standard esprit for overcoming imperfections in doa estimation[C]. In: ICASSP 2021-2021 IEEE International Conference on Acoustics, Speech and Signal Processing (ICASSP), pp. 4375–4379 (2021). IEEE
12. Qian, C.: A simple modification of esprit[J]. IEEE Signal Processing Letters **25**(8), 1256–1260 (2018)
13. Akkar, S., Harabi, F., Gharsallah, A.: Linear esprit-like algorithms for fast directions of arrival estimation with real structure[C]. In: 2019 IEEE 19th Mediterranean Microwave Symposium (MMS), pp. 1–4. IEEE
14. Zheng, Z., Huang, Y., Wang, W.-Q., So, H.C.: Direction-of-arrival estimation of coherent signals via coprime array interpolation[J]. IEEE Signal Processing Letters **27**, 585–589 (2020)
15. Li, X., Zhang, W.: Doa estimation using virtual esprit with successive baselines and coprime baselines[J]. Circuits, Systems, and Signal Processing **40**(4), 2065–2075 (2021)
16. Van Doan, S., Tran, T.C., *et al.*: Doa estimation of underwater acoustic signals using non-uniform linear arrays[J]. In: International Conference on Industrial Networks and Intelligent Systems, pp. 103–110 (2018). Springer
17. Ding, J., Yang, M., Chen, B., Yuan, X.: A single triangular ss-emvs aided high-accuracy doa estimation using a multi-scale l-shaped sparse array[J]. EURASIP Journal on Advances in Signal Processing **2019**(1), 1–15 (2019)
18. Zheng, Z., Mu, S.: Two-dimensional doa estimation using two parallel nested arrays[J]. IEEE Communications Letters **PP**(99), 1–4 (2019)
19. Xi, N., Li, L.: A computationally efficient subspace algorithm for 2-d doa estimation with l-shaped array[J]. IEEE Signal Processing Letters **21**(8), 971–974 (2014)

20. Ning, G., Wang, B., Zhou, C., Feng, Y.: A velocity independent music algorithm for doa estimation[C]. In: 2017 IEEE International Conference on Signal Processing, Communications and Computing (ICSPCC), pp. 1–4 (2017). IEEE
21. Ning, G., Jing, G., Li, X., Zhao, X.: Velocity-independent and low-complexity method for 1d doa estimation using an arbitrary cross-linear array[J]. EURASIP Journal on Advances in Signal Processing **2020**(1), 1–9 (2020)
22. Kay, S.M.: Fundamentals of Statistical Signal Processing: Estimation Theory[M], pp. 20–46 (1993)
23. Pal, P., Vaidyanathan, P.P.: Nested arrays: A novel approach to array processing with enhanced degrees of freedom[J]. IEEE Transactions on Signal Processing **58**(8), 4167–4181 (2010)